Eur. Phys. J. B **52**, 209–218 (2006)
DOI: 10.1140/epjb/e2006-00281-y

THE EUROPEAN PHYSICAL JOURNAL B

Antiferromagnetic Ising spin glass competing with BCS pairing interaction in a transverse field

S.G. Magalhães[1,a], F.M. Zimmer[1], C.J. Kipper[1], and E.J. Calegari[1]

Laboratório de Mecânica Estatística e Teoria da Matéria Condensada (PPGFIS-Dep. Física) - UFSM, 97105-900 Santa Maria, RS, Brazil

Received 29 March 2006
Published online 7 July 2006 –

Abstract. The competition among spin glass (SG), antiferromagnetism (AF) and local pairing superconductivity (PAIR) is studied in a two-sublattice fermionic Ising spin glass model with a local BCS pairing interaction in the presence of an applied magnetic transverse field Γ. In the present approach, spins in different sublattices interact with a Gaussian random coupling with an antiferromagnetic mean J_0 and standard deviation J. The problem is formulated in the path integral formalism in which spin operators are represented by bilinear combinations of Grassmann variables. The saddle-point Grand Canonical potential is obtained within the static approximation and the replica symmetric ansatz. The results are analysed in phase diagrams in which the AF and the SG phases can occur for small g (g is the strength of the local superconductor coupling written in units of J), while the PAIR phase appears as unique solution for large g. However, there is a complex line transition separating the PAIR phase from the others. It is second order at high temperature that ends in a tricritical point. The quantum fluctuations affect deeply the transition lines and the tricritical point due to the presence of Γ.

PACS. 05.50.+q Lattice theory and statistics – 64.60.Cn Order-disorder transformations; statistical mechanics of model systems

1 Introduction

It is now well-established that strongly correlated systems such as heavy fermions (HF) [1] and high temperature superconductors (HTSC) [2], upon doping, can present magnetic order or superconductivity. The complexity involved in such physical systems as, for instance, the existence of Non-Fermi Liquid (NFL) behaviour, has given rise to new theoretical approaches. In particular, recent works have proposed that the presence of disorder can affect these strongly correlated systems (see [3] and references therein) being even source of NFL behaviour, for example, in HF [4,5]. The presence of disorder can also induce frustration which, in fact, has been found in several HF [6–9] and HTSC [10,11] physical systems. Some theories have been investigating whether or not spin glass (SG) phase can be found in models designed to study certain aspects of HF or HTSC systems [12–14]. For instance, the existence of a SG solution has been demonstrated in the Kondo lattice model [15,16]. Nevertheless, relatively little consideration [17] has been given in order to obtain the behaviour of the transition temperatures for these strongly correlated physical systems and, thus, to mimic the phase boundaries of their global phase diagram which includes antiferromagnetism (AF), SG, superconductivity and the possible presence of a Quantum Critical Point (QCP).

Regarding the experimental scenario, there are some similarities in the global phase diagrams between some HF and HTSC, although the microscopical mechanisms involved in such systems are different [18]. For instance, the HTSC compound $Y_{1-x}Ca_xBa_2Cu_3O_6$ has a phase diagram temperature T versus the hole concentration p_{sh} [10] which displays an AF ordering for low p_{sh}. The respective Néel temperature T_N decreases for $0 < p_{sh} < 0.035$ until the onset of a second transition at T_f in which is found the superposition of frustration with a preformed AF background. For $p_{sh} > 0.035$, there is another transition from the previous mixed state to a pure SG. The SG transition temperature T_g also decreases with the increase of p_{sh} until the onset of superconductivity (SC). However, the SG regime is still found into the SC region. For instance, for $0.06 < p_{sh} < 0.10$ there is still traces of spin freezing. Finally, for large values of p_{sh}, the superconductivity is dominant. From the side of the HF systems, the example is the compound $U_{1-x}La_xPd_2Al_3$. When the doping of La is increased, the corresponding phase diagram shows the AF ordering to be replaced by a SG state in the region $0.25 \leq x \leq 0.65$. At $x = 1$, the system is a superconductor. The Néel temperature T_N is sharply decreased from $T = 14.6$ K until $T = 2.6$ K when x increases, while the

[a] e-mail: ggarcia@ccne.ufsm.br

subsequent SG transition temperature T_g drops to a QCP at $x \approx 0.8$. In the intermediated doping region between the QCP and $x = 1$, a NFL behaviour is observed.

In the last years, several works have been studying the competition between SG and pairing formation in a formulation where the spins are represented as bilinear combination of fermionic creation and destruction operators [19–21]. The model used in such approaches is composed of a random Gaussian coupling between localized spins together with pairing interaction in the real space. In fact, it can be shown that both terms of this simple model have the same origin. They can be derived by eliminating the conduction electrons, in second order of perturbation (see Appendix in Ref. [19]), from an earlier model introduced to treat conventional superconductor doped with magnetic impurities [22]. A saddle-point solution for the respective grand-canonical potential has been obtained within functional integral formalism for the Ising [19] and the Heisenberg [20] version of the model in the half-filled situation using the static approximation [23] and the replica symmetry ansatz. For the Ising case, the phase diagram temperature versus the strength of the pairing coupling g (in units of J that is the variance of the Gaussian random distributed spin-spin coupling) displays two phase boundaries. For lower g, it is found a second order line transition between paramagnetism (NP) and SG at $T_g = 0.95\ J$. For large g, there is a complex line transition $T_1(g)$ separating the PAIR phase (where pair formation is found) from the SG and NP phases. The line transition $T_1(g)$ is a second order for high temperature when the boundary is between NP and the PAIR phase. However, it becomes first order at lower temperature. The corresponding tricritical point T_{trict} has been located on $T_1(g)$ above of T_g. As consequence, the boundary between SG and the PAIR phase is entirely first order. Weak hopping corrections done elsewhere [21] demonstrated that the phase boundaries described previously with no hopping are essentially maintained.

The model in reference [19] has two important shortcomings. The first one is the lack of quantum spin flipping mechanism which would be able to suppress the transition temperatures leading them to a QCP. Even the Heisenberg extension of the problem [20] has been unable to produce a QCP. This particular weakness has been corrected in reference [24] by the addition of a transverse field Γ in the Ising version of the model. The presence of Γ has changed the behaviour of both transition temperatures T_g and $T_1(g)$. As long Γ increases, the first one moves downwards in the direction of a QCP while the second one is displaced. Therefore, Γ has also suppressed the PAIR solution in the sense that it is necessary larger values of the pairing coupling strength g to find the PAIR solution [24]. The tricritical point T_{trict} is affected by the presence of Γ. The transverse field moves up T_{trict} which enlarges the first order portion of $T_1(g)$. Finally, it has been proposed a relationship between Γ and g (J is kept constant) based on the argument that the pairing and RKKY interaction have the same origin in the derivation of the model [19]. As consequence, the effects described previously are superposed in a single phase diagram T versus g due to the increase of g, hence Γ. It shows T_g decreasing towards a QCP at $g = g_c$, then a PAIR phase can be found at $g > g_c$ with T_{trict} located at higher values of T and g than the case $\Gamma = 0$.

Nevertheless, the model used in references [19–21] has a second shortcoming, it is unable to produce an AF solution. Thus, the model is useless if one is trying to study the phase boundaries which include SG, PAIR phase and also AF. However, quite recently the competition between AF and SG has been analysed in a disordered two-sublattice fermionic spin model. The model is a Gaussian random coupling with an antiferromagnetic mean J_0 and standard deviation J between spins in distinct sublattices with the presence of a transverse Γ and parallel H magnetic fields [25]. In fact, it is the fermionic version of the model introduced by Korenblit and Shender (KS) [26] which is used to study the competition between AF and SG with classical Ising variables. This classical two-sublattice model has itself unexpected effects as compared with the classical single lattice SG Ising model [27]. For example, opposite solutions are enforced by the degree of frustration $(J_0)^{-1}$ and H (given in units of J). When degree of frustration decreases the AF solution is favored, while the field H can eventually enhance the frustration in a certain range [26]. This last effect is related with the asymmetry between the two-sublattice due the coupling with H. The presence of the Γ in the fermionic version of KS model has introduced important differences if compared with its classical counterparts as long there is a competing mechanism associated with J_0, H and Γ [25]. For instance, Γ suppresses the magnetic orders leading their critical temperatures to QCPs, while H can favour frustration at the same time that it destroys the AF phase.

Therefore, the purpose of the present work is to study the competition among AF, SG and the PAIR phase using the fermionic Ising KS model with a local pairing interaction in each sublaticce in the presence of a transverse field Γ. Particularly, the focus is to describe the behaviour of the possible transition temperatures present in the problem. We follow the same approach used in references [19,20,24]. The partition function is obtained in the functional integral formalism where the spin operators are given as bilinear combinations of Grassmann fields. The static approximation (SA) and the replica symmetry (RS) ansatz are used to calculate the saddle-point Grand canonical potential. Particularly, we extend for the present two-sublattice problem a procedure that mixes Nambu matrices and spinors as already introduced in reference [24]. The stability of the RS solution is also investigated. Surely, the simple model used in the present work is not suited to describe the extremely complicate physics present in HF as well as in HTSC systems. However, it can be, at least, useful to mimic general features of a phase diagram in which AF, SG, pairing coupling and a quantum spin flipping mechanism are present.

The use of SA and RS ansatz deserves some remarks. It is well-known the SA is not adequate to describe the low temperature behaviour of the spin-spin correlation

function [23]. However, the justification for the use of the SA in this work is based on the fact that our interest is mainly to obtain the possible transition temperatures associated with AF, SG and PAIR competition. The analysis of the quantum rotor model in the $M \to \infty$ indicates that the critical line can be obtained from the zero frequency mode [28].

Although the focus in this work is to obtain the phase boundaries of the fermionic version of KS model with a pairing interaction in the presence of a transverse field Γ, the thermodynamics is not the only source of valuable information. In the case of Ising SG fermionic model, other physical quantities can have an interesting behaviour. For example, the density of states (DOS) and, hence, the local Green's function are affected at low temperature by the replica symmetry breaking [30]. In particular, there is a presence of a pseudogap. Recently, a mapping between the one-lattice fermionic Ising SG and the classical Ghatak-Sherrington model [31] has demonstrated that the true origin of such effects in the DOS are, in fact, classical [32]. However, for the present model we can speculate if there is such kind of mapping due to the presence of the transverse field. In that sense, this work can be also thought as a first step towards the understanding of the problem given by the model introduced here from a many-body perspective since the thermodynamics is well understood, at least, at mean field level.

This paper presents the following structure. In Section 2, we derive the saddle-point Grand Canonical potential and the set of equations for the order parameters which is enlarged when compared with a single lattice Ising model studied in reference [24]. In Section 3, we solve the order parameter equations. In order to capture properly the competition among the phases present in the problem, we build up phase diagrams T versus g for several values of Γ and J_0 given in units of J where J_0 and J are the mean and standard deviation of the random Gaussian spin-spin interlattice coupling, respectively. On the other hand, the effects of the transverse field Γ are better shown in a phase diagram T versus Γ for constant values of g and J_0. We also obtain a phase diagram T versus g in which Γ and J_0 are related with g based on the same arguments proposed in reference [24]. This procedure mixes the effects of both parameters in the phase diagram. In the last section, we make our conclusions.

2 General formulation

The model studied here is composed by interlattice Gaussian random spin-spin interaction [26], a intrasite local BCS pairing interaction (which favors double occupation of sites in each sublattice) with a transverse magnetic field applied Γ. Therefore, the Hamiltonian is given by:

$$H = -\sum_{i_a j_b} J_{i_a j_b} S^z_{i_a} S^z_{j_b} - 2\Gamma \sum_p \sum_{i_p=1}^{N} S^x_{i_p} - \frac{g}{N} \sum_p \sum_{i_p j_p} c^\dagger_{i_p\uparrow} c^\dagger_{i_p\downarrow} c_{j_p\downarrow} c_{j_p\uparrow} \quad (1)$$

where the sums over i_p (j_p) are run over the N sites of each sublattice p ($p = a$ or b). The exchange interaction $J_{i_a j_b}$ is an independent random variable with the following Gaussian distribution:

$$P\left(J_{i_a j_b}\right) = \sqrt{\frac{N}{64\pi J^2}} \exp\left[-\frac{\left(J_{i_a j_b} + \frac{4}{N} J_0\right)^2}{\frac{64 J^2}{N}} \right]. \quad (2)$$

The spin operators in equation (1) are defined in terms of fermion operators:

$$S^z_{i_p} = \frac{1}{2}\left[\hat{n}_{i_p\uparrow} - \hat{n}_{i_p\downarrow}\right], \quad S^x_{i_p} = \frac{1}{2}\left[c^\dagger_{i_p\uparrow} c_{i_p\downarrow} + c^\dagger_{i_p\uparrow} c_{i_p\downarrow}\right] \quad (3)$$

where $\hat{n}_{i_p\sigma}$ gives the number of fermions at site i_p with spin projection $\sigma = \uparrow$ or $\downarrow$. $c^\dagger_{i_p\sigma}$ and $c_{i_p\sigma}$ are the fermion creation and annihilation operators, respectively.

The problem is formulated in a path integral formalism in which the spin operators are represented as anticommuting Grassmann fields (ϕ^*, ϕ). Therefore, the Grand canonical partition function is given by:

$$Z = \int D[\phi^*\phi] \exp[A] \quad (4)$$

with the action

$$A = \int_0^\beta d\tau \Bigg\{ \sum_{p,\sigma} \sum_{i_p} \left[\phi^*_{i_p\sigma}(\tau) \left(\frac{\partial}{\partial\tau} - \mu \right) \phi_{i_p\sigma}(\tau) \right] - H(\phi^*(\tau), \phi(\tau)) \Bigg\}, \quad (5)$$

$\beta = 1/T$ (T is the temperature), τ is a complex time and μ is the chemical potential. The Fourier decomposition of the time-dependent quantities is employed in equation (5). The action can be write as $A = A_\Gamma + A_{SG} + A_{BCS}$ with:

$$A_\Gamma = \sum_p \sum_{i_p} \sum_w \underline{\phi}^\dagger_{i_p}(\omega) [i\omega + \beta\mu + \beta\Gamma \underline{\sigma}^x] \underline{\phi}_{i_p}(\omega), \quad (6)$$

$$A_{SG} = \sum_{i_a j_b} \sum_{\omega'} \beta J_{i_a j_b} S^z_{i_a}(\omega') S^z_{j_b}(-\omega'), \quad (7)$$

$$S^z_{i_p}(\omega') = \frac{1}{2} \sum_\omega \underline{\phi}^\dagger_{i_p}(\omega + \omega') \underline{\sigma}^z \underline{\phi}_{i_p}(\omega), \quad (8)$$

$$A_{BCS} = \frac{\beta g}{N} \sum_p \sum_{i_p j_p} \sum_{\omega'} \rho^*_{i_p}(\omega') \rho_{i_p}(\omega') \quad (9)$$

where $\rho_{i_p}(\omega') = \sum_w \phi_{i_p\downarrow}(-\omega)\phi_{i_p\uparrow}(\omega' + \omega)$, $\underline{\sigma}^\upsilon$ ($\upsilon = x,\ y$ or z) denotes the Pauli matrices, $\underline{\phi}^\dagger_{i_p} = (\phi^*_{i_p\uparrow}(\omega)\ \ \phi^*_{i_p\downarrow}(\omega))$ is a Grassmann spinor, and $\omega = (2m+1)\pi$ and $\omega' = m\pi$ ($m = 0, \pm 1, ...$) are the Matsubara's frequencies.

The grand canonical potential is obtained within the static approximation which considers $\omega' = 0$ in equations (7)–(9) [24,25]. The configurational averaged thermodynamic potential per site is obtained with the

use of the replica method: $\beta\Omega = -\frac{1}{N}\langle \ln Z\{y\}\rangle_{J_{ij}} = -\frac{1}{2N}\lim_{n\to 0}(\langle Z^n\rangle_{J_{ij}} - 1)/n$ where the replicated partition function is:

$$\langle Z^n\rangle_{J_{ij}} = \int \prod_{\alpha} D(\phi^{*\alpha}\phi^{\alpha}) \exp\left[A^{\alpha}_{\Gamma} + A^{st}_{SG} + A^{st}_{BCS}\right] \tag{10}$$

where A^{α}_{Γ} is given by equation (6) with a sub-index α,

$$A^{st}_{SG} = \sum_{i_a j_b}\left[\frac{8\beta^2 J^2}{N}\left(\sum_{\alpha} S^{\alpha}_{i_a} S^{\alpha}_{j_b}\right)^2 - \frac{2\beta J_0}{N}\sum_{\alpha} S^{\alpha}_{i_a} S^{\alpha}_{j_b}\right] \tag{11}$$

$$A^{st}_{BCS} = \frac{\beta g}{4N}\sum_{\alpha,p}\sum_{\upsilon=x,y}\left[\sum_{i_p}\sum_{w} \underline{\phi}^{'\alpha\dagger}_{i_p}(\omega)\underline{\sigma}^{\upsilon}\underline{\phi}^{'\alpha}_{i_p}(\omega)\right]^2 \tag{12}$$

with the replica index α running from 1 to n. In equation (12), it is introduced the Nambu matrices $\underline{\phi}^{'\alpha\dagger}_{j}(\omega)$ and $\underline{\phi}^{'\alpha}_{j}(\omega)$ in which $\underline{\phi}^{'\alpha\dagger}_{j}(\omega) = (\phi^{*\alpha}_{j\uparrow}(\omega)\ \phi^{\alpha}_{j\downarrow}(-\omega))$.

Equation (11) can be rearranged reviewing the sums over different sublattices by square sums over the same sublattice. The replicated partition function is then linearized by using Hubbard-Stratonovich transformations. It inserts the replica-dependent auxiliary fields $q^{\alpha\beta}_{p}$, m^{α}_{p}, $\eta^{\alpha}_{R,p}$ and $\eta^{\alpha}_{I,p}$ in equation (10). The Gaussian integrals over these fields have been exactly performed in the thermodynamic limit by the steepest descent method. Therefore, the Grand canonical potential is:

$$\mathcal{Z}(n)/N = \beta g\sum_{\alpha,p}|\eta^{\alpha}_{p}|^2 - \beta J_0\sum_{\alpha} m^{\alpha}_{a} m^{\alpha}_{b} + \beta^2 J^2\sum_{\alpha\beta} q^{\alpha\beta}_{a} q^{\alpha\beta}_{b} - \ln \Lambda^{a}_{\alpha\beta}\Lambda^{b}_{\alpha\beta} \tag{13}$$

where $\eta^{\alpha}_{p} = \eta^{\alpha}_{R,p} + i\eta^{\alpha}_{I,p}$ and

$$\Lambda^{p}_{\alpha\beta} = \int \prod_{\alpha} D[\phi^{*\alpha}_{p}\phi^{\alpha}_{p}] \exp\left[4\beta^2 J^2\sum_{\alpha\beta} q^{\alpha\beta}_{p'} S^{\alpha}_{p} S^{\beta}_{p} - 2\beta J_0\sum_{\alpha} m^{\alpha}_{p'} S^{\alpha}_{p} + A^{\alpha}_{\Gamma,p} + \beta g\sum_{\omega,\alpha}\underline{\phi}^{'\dagger\alpha}_{p}\underline{\eta}^{\alpha}_{p}\underline{\phi}^{'\alpha}_{p}\right] \tag{14}$$

with the matrix $\underline{\eta}^{\alpha}_{p} = \eta^{\alpha}_{R,p}\underline{\sigma}^{x} + \eta^{\alpha}_{I,p}\underline{\sigma}^{y}$. The fields $q^{\alpha\beta}_{p}$, m^{α}_{p} and $|\eta^{\alpha}_{p}|$ in equation (13) are given by saddle-point equations, in which $q^{\alpha\beta}_{p}$ is related with the spin glass order parameter, m^{α}_{p} is the magnetization of the sublattice p, and $|\eta^{\alpha}_{p}|$ is an order parameter that indicates long range order where there is double occupation of sites in sublattice p.

In the present work, it is assumed the replica symmetric ansatz, which considers $q^{\alpha\beta}_{p} = q_p$ for all $\alpha \neq \beta$, $q^{\alpha\alpha}_{p} = \overline{q}_p = \bar{\chi}_p + q_p$, $m^{\alpha}_{p} = m_p$, and $\eta^{\alpha}_{p} = \eta_p$ for all α. The physical quantity $\beta\bar{\chi}_p$ is the static susceptibility when $J_0 = 0$. The sums over replica indices are performed. It produces quadratic terms in equation (14) that are linearized introducing new auxiliary fields in equation (13). The resulting functional Grassmann integral is an exponential that sums quadratic forms of spinors and Nambu matrices. In order to perform the integral over the Grassmann fields, it can be used a matrix that mixes elements of spinors and Nambu matrices, such as:

$$\Lambda^{p}_{\alpha\beta} = \int Dz_p\left\{\int D\xi_p \mathcal{I}(z_p,\xi_p)\right\}^n \tag{15}$$

where $Dx = dx\mathrm{e}^{-x^2/2}/\sqrt{2\pi}$ ($x = \xi_p$ or z_p),

$$\mathcal{I}(z_p,\xi_p) = \int D[\phi^{*}_{p}\phi_p]\exp\left[\sum_{\omega}\underline{\Phi}^{\dagger}_{p}(w)\underline{G}^{-1}_{p}(w)\underline{\Phi}_{p}(w)\right] \tag{16}$$

with

$$\underline{\Phi}^{\dagger}_{p}(w) = \left[\phi^{*}_{p\uparrow}(w)\quad \phi^{*}_{p\downarrow}(w)\quad \phi_{\downarrow p}(-w)\quad \phi_{p\uparrow}(-w)\right], \tag{17}$$

$$\underline{G}^{-1}_{p}(\omega) = \begin{pmatrix} i\omega+\zeta^{+} & \beta\Gamma & \beta g\eta_p & 0 \\ \beta\Gamma & i\omega+\zeta^{-} & 0 & -\beta g\eta_p \\ \beta g\eta^{*}_{p} & 0 & i\omega-\zeta^{+} & -\beta\Gamma \\ 0 & -\beta g\eta^{*}_{p} & -\beta\Gamma & i\omega-\zeta^{-} \end{pmatrix} \tag{18}$$

and $\zeta^{\pm} = \beta\mu_p \pm \beta h_p$. The internal field $h_p = J(\sqrt{2q_{p'}}z_p + \sqrt{2\bar{\chi}_{p'}}\xi_p) - J_0 m_{p'}$, which acts on the sublattice p, depends on the order parameters of sublattice $p^{'}$ ($p^{'} \neq p$) [25].

The functional integral in equation (16) and the sum over the Matsubara's frequencies can be performed:

$$\mathcal{I}(z_p,\xi_p) = \cosh\beta\sqrt{\mu^2 + g^2\eta^2_p} + \cosh\beta\sqrt{\Delta_p} \tag{19}$$

with $\Delta_p = h^2_p + \Gamma^2$. This result and equation (13) are used to express the thermodynamic potential as:

$$2\beta\Omega = -\beta J_0 m_a m_b + \beta^2 J^2(\bar{\chi}_a\bar{\chi}_b + \bar{\chi}_a q_b + \bar{\chi}_b q_a) + \beta g(\eta^2_a + \eta^2_b) - \sum_{p=a,b}\int_{-\infty}^{\infty} Dz_p \ln K_p(z_p) + \ln 4 \tag{20}$$

where

$$K_p(z_p) = \left(\cosh\beta g\eta_p + \int_{-\infty}^{\infty} D\xi_p \cosh\beta\sqrt{\Delta_p}\right) \tag{21}$$

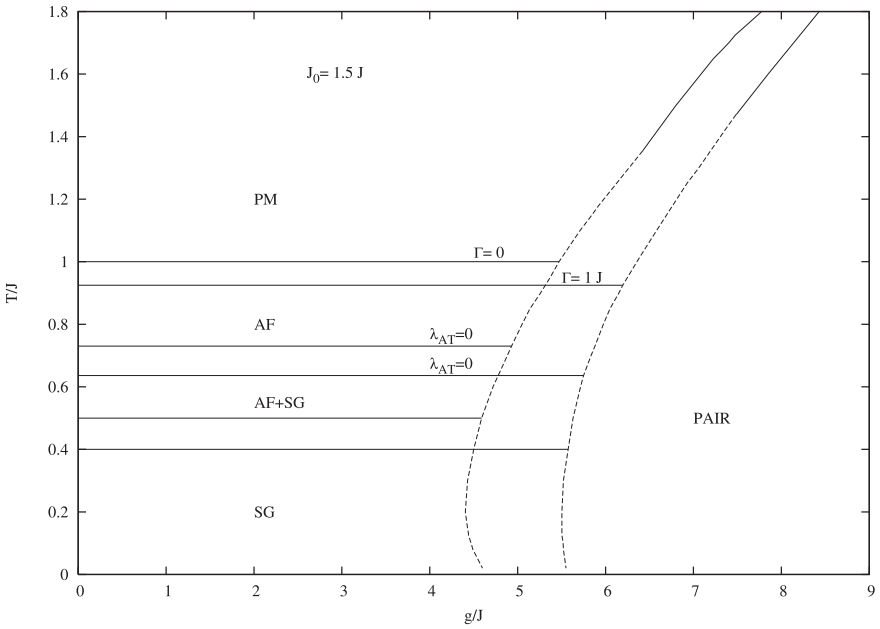

Fig. 1. Phase diagrams as a function of T/J and pairing coupling g/J for $J_0 = 1.5\ J$ and for two values of Γ/J: $\Gamma = 0$ and $\Gamma = 1\ J$. The full lines indicate second-order transitions while the dashed lines indicate first-order transitions.

with $\mu = 0$ to ensure the half-filling situation. The order parameters are given by the extreme condition of equation (20):

$$m_p = \int_{-\infty}^{\infty} Dz_p \frac{\int_{-\infty}^{\infty} D\xi_p \frac{h_p}{\sqrt{\Delta_p}} \sinh \beta\sqrt{\Delta_p}}{K_p(z_p)} \tag{22}$$

$$\eta_p = \frac{1}{2}\int_{-\infty}^{\infty} Dz_p \frac{\sinh(\beta g \eta_p)}{K_p(z_p)} \tag{23}$$

$$q_p = \int_{-\infty}^{\infty} Dz_p \left[\frac{\int_{-\infty}^{\infty} D\xi_p \frac{h_p}{\sqrt{\Delta_p}} \sinh \beta\sqrt{\Delta_p}}{K_p(z_p)}\right]^2 \tag{24}$$

$$\bar{\chi}_p = \int_{-\infty}^{\infty} Dz_p \frac{\int_{-\infty}^{\infty} D\xi_p \frac{1}{\beta^2}\frac{\partial^2}{\partial h_p^2} \cosh \beta\sqrt{\Delta_p}}{K_p(z_p)} - q_p. \tag{25}$$

The stability of replica symmetric solution is analysed by Almeida-Thouless eigenvalue λ_{AT}:

$$\lambda_{AT} = 1 - 4(\beta J)^4 \prod_p \int_{-\infty}^{\infty} Dz_p \left(\frac{I_p(z_p)}{(K_p(z_p))^2}\right)^2 \tag{26}$$

where

$$I_p(z_p) = K_p(z_p)\int_{-\infty}^{\infty} D\xi_p \frac{1}{\beta^2}\frac{\partial^2}{\partial h_p^2}\cosh\beta\sqrt{\Delta_p} - \left(\int_{-\infty}^{\infty} D\xi_p \frac{h_p}{\sqrt{\Delta_p}}\sinh\beta\sqrt{\Delta_p}\right)^2. \tag{27}$$

3 Phase diagrams

Numerical investigations of the order parameter equations (22–25) allow us to find three kinds of solutions. The SG solution corresponds to $q_a = q_b \neq 0$ (with $m_a = m_b = 0$, $\eta_a = \eta_b = 0$) while the AF solution is $m_a = -m_b \neq 0$ (with $q_a = q_b \neq 0$, $\eta_a = \eta_b = 0$). The spin pairing solution (PAIR phase) corresponds to η_a and η_b different from zero while the rest of order parameters is zero. The instability of the replica symmetry (RS) solution of the SG is also investigated which allows us to identify the presence of a mixed phase AF+SG. This mixed phase corresponds to a replica symmetry breaking (RSB) SG with $m_p \neq 0$ ($p = a, b$) [24]. The emergence of each type of solution depends on the relationship among parameters g, $(J_0)^{-1}$ (the degree of frustration) and Γ given in units of J.

Therefore, we can build, in the beginning, two kinds of phase diagrams T (T is the temperature) versus: (a) g (g is the strength of intrasite pairing interaction) with J_0 and Γ kept independents; (b) Γ with g and J_0 kept independents. The first phase diagram can show directly the competition among AF, SG and PAIR phases. The second one gives more precise information about the role of the transverse field on the transition lines present in the problem.

In Figure 1, we show the results for T versus g for $J_0 = 1.5\ J$ with $\Gamma = 0$ and J. Therefore, in the region of small g in Figure 1, it is quite clear that the parameter J_0 is related with the presence of magnetic solutions. Firstly, the AF solution appears below T_{N}. Then, when temperature is decreased, there is the onset of a mixed phase AF+SG at T_f. Finally, at lower temperature, there is a transition from AF+SG to a SG phase at T_g. The three magnetic transition lines mentioned above are second order. For large g, the solutions found for the order parameters indicate the existence of the PAIR phase [19,20,24] in which there is pairing formation in both sublattices. The role of the transverse field Γ is also clear in this particular phase diagram. The field decreases simultaneously the

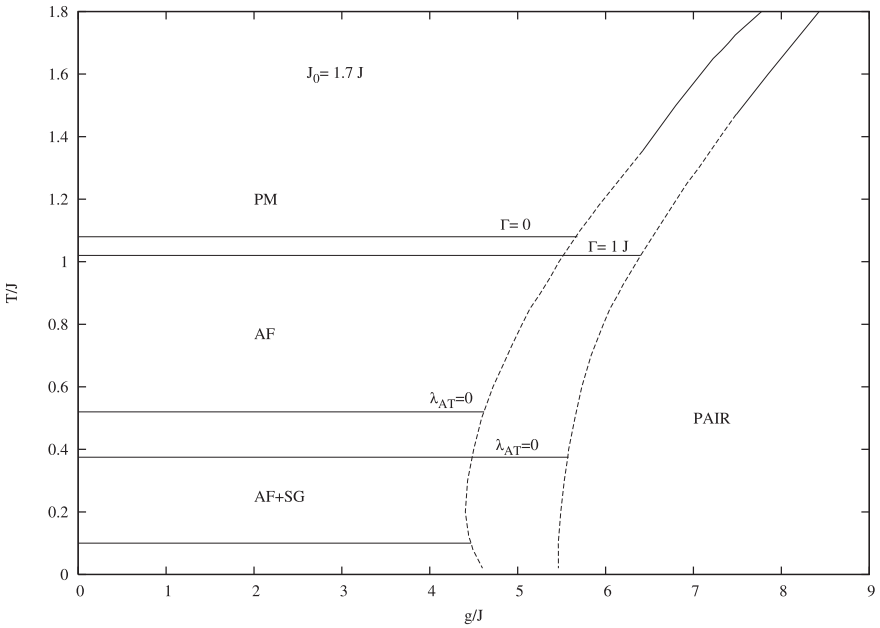

Fig. 2. Phase diagrams as a function of T/J and pairing coupling g/J for $J_0 = 1.7\ J$ and for two values of Γ/J: $\Gamma = 0$ and $\Gamma = 1\ J$. It is used the same convention as Figure 1 for the transition lines.

magnetic transition temperatures $T_{\rm N}$, T_f and T_g. It also displaces the PAIR transition line $T_1(g)$ in the sense that it is necessary to increase the parameter g to find a PAIR solution in the problem.

Figure 2 shows the previous phase diagrams when the degree of frustration is decreased ($J_0 = 1.7\ J$) with the transverse field kept $\Gamma = 0$ and J. We can compare the results in the small and large g region in this figure with the phase diagram given in Figure 1. The conclusion is direct, in the small g region, there are competing effects due to J_0 and Γ [25]. The decrease of the degree of frustration enhances $T_{\rm N}$. However, it decreases T_f and T_g as well. On the other hand, the whole set of magnetic transition temperatures $T_{\rm N}$, T_f and T_g decreases with Γ. The superposition of both effects is responsible by the suppression of the SG phase in Figure 2. The line transition $T_1(g)$ is not affected by the change of the degree of frustration $(J_0)^{-1}$ while the transverse field Γ has the same role as before, it displaces $T_1(g)$.

The numerical analyses indicate that the PAIR transition line $T_1(g)$ is more complicated than the magnetic ones. It is a second order phase transition at higher temperatures and a first one at lower temperatures, where there are multiple PAIR solutions. In this case, the stable solution minimazes the thermodynamic potential. This same criterion is used to obtain the first-order boundary. The transition lines can be also analysed by performing a Landau expansion of the thermodynamic potential in powers of the order parameters (q_a, q_b, m_a, m_b, η_a and η_b). We can explore the symmetry of the parameters: $q = q_a = q_b$, $\bar{\chi} = \bar{\chi}_a = \bar{\chi}_b$, $\eta = \eta_a = \eta_b$ and $m_a = -m_b$. Equation (20) is expanded in powers of q, η and $l = (m_a - m_b)/2$ (l is the antiferromagnetic order parameter), while $\bar{\chi}(q, l, \eta)$ is given by the saddle-point equation (25). After some lengthy calculations, the Landau expansion of the thermodynamic potential is:

$$2\beta\Omega = \beta^2 J^2 \bar{\chi}_0 - 2\ln K_0 + A_2 l^2 + B_2 q^2 + C_2\eta^2 + C_4\eta^4 \quad (28)$$

with

$$A_2 = 4\beta J_0(1 - \beta J_0 \bar{\chi}_0) l^2 \quad (29)$$

$$B_2 = -\frac{\beta^2 J^2}{2!} + \beta^4 J^4 \bar{\chi}_0^2, \quad (30)$$

$$C_2 = \beta g - \frac{\beta^2 g^2}{2K_0}, \quad (31)$$

$$C_4 = \frac{\beta^4 g^4}{4! K_0^2}\left(\frac{3J^2}{g^2} K_0 \bar{\chi}_0 \bar{\chi}_2 + 3 - K_0\right) \quad (32)$$

where $K_0 = 1 + \int_{-\infty}^{\infty} D\xi \cosh\sqrt{\Delta_0}$,

$$\bar{\chi}_0 = \frac{1}{K_0}\int_{-\infty}^{\infty} D\xi \xi^2 \frac{\sinh\sqrt{\Delta_0}}{\sqrt{\Delta_0}}, \quad (33)$$

$$\bar{\chi}_2 = \frac{-\beta^2 g^2 \bar{\chi}_0/K_0}{1 + \beta^2 J^2[\bar{\chi}_0^2 - \int D\xi \xi^4 (\frac{\cosh\sqrt{\Delta_0}}{\Delta_0} - \frac{\sinh\sqrt{\Delta_0}}{\Delta_0})/K_0]} \quad (34)$$

and $\Delta_0 = 2\beta^2 J^2 \bar{\chi}_0 \xi^2 + \beta^2 \Gamma^2$. The tricritical point T_{tricl} can be obtained from equations (31–32) which show that the transverse field Γ affects the location of the T_{tricl}. Actually, it moves upwards T_{tricl} (see Figs. 1 and 2) [20,24].

In Figure 3, we show the phase diagram T versus Γ for $J_0 = 1.5\ J$ and $g = 0, 6.5\ J$, $8\ J$ and $9\ J$. The case in which there is no pairing coupling is shown in Figure 3a. In fact, this situation has been studied in reference [25] where the increase of Γ leads the transition temperatures $T_{\rm N}$, T_f and

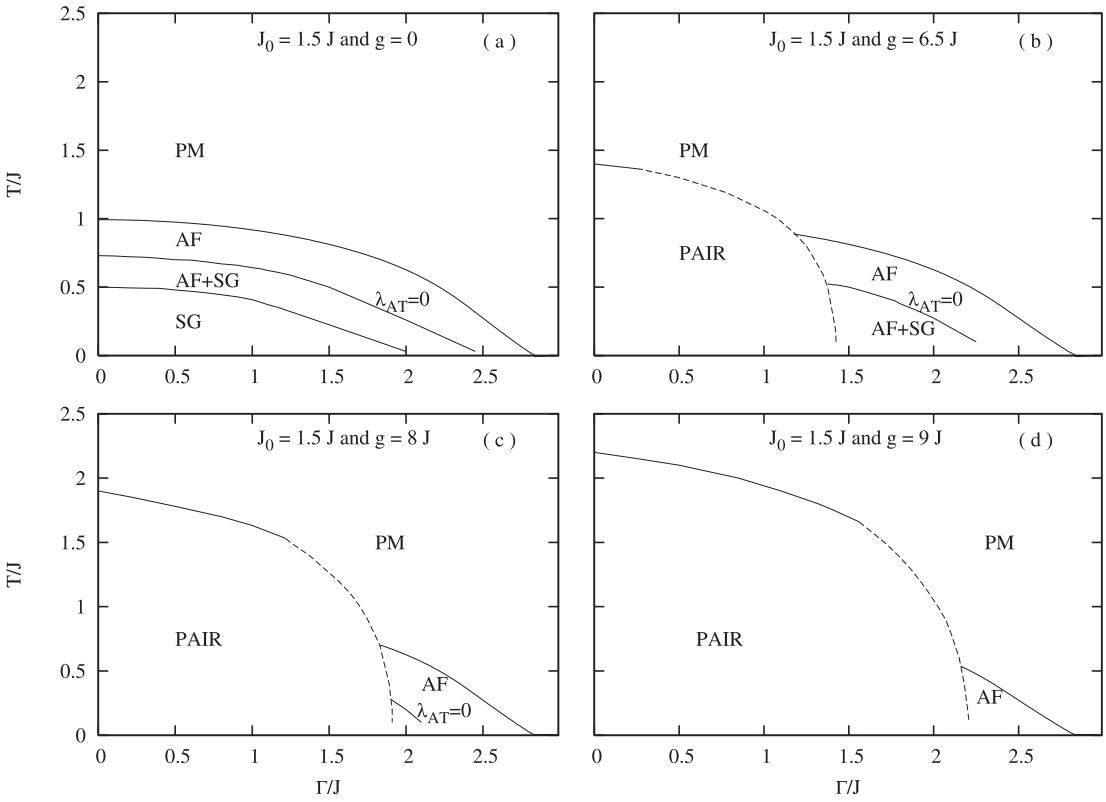

Fig. 3. Phase diagrams as a function of T/J and Γ/J for $J_0 = 1.5\ J$ and several fixed values of g/J: (a) $g = 0$, (b) $g = 6.5\ J$, (c) $g = 8.0\ J$ and (d) $g = 9.0\ J$. It is used the same convention as Figure 1 for the transition lines.

T_g towards their respective QCP's. In particular, the critical transverse field for AF transition can be obtained analytically by expanding the sublattice magnetization m_p (see Ref. [25]). The ordering $T_g < T_f < T_{\rm N}$ is kept when Γ increases, which is the reason why the transition temperatures $T_{\rm N}$, T_f and T_g are simultaneously depressed in Figures 1 and 2. The increase of g (see Figs. 1b, 1c, 1d) allows the existence of a PAIR solution which depends on, as discussed in reference [24], of the ratio Γ/g as well as the existence of a magnetic solution depends on Γ/J_0 in the present work. From this view point, the role of Γ in Figures 1 and 2 is clearly confirmed in Figure 3, it tends to suppress any phase which is appearing as solution in the problem. Actually, the displacement of the PAIR phase in Figures 1 and 2, when Γ increases, reflects this effect. Moreover, the increase of g also leads (if J_0 is kept constant) the PAIR phase to become dominant. It also moves upward the tricritical point T_{trict} as in reference [24].

The information contained in Figures 1–3 can be displayed in a more adequate format if we assume a relationship among the parameters Γ, J_0 and g. This kind of procedure has already been adopted in reference [24], which is ultimately justified by the fact that both RKKY and the pairing interaction in equation (1) are originated from the same source [19]. In the present case, Γ would have the equivalent role of spin flipping part of the Heisenberg model [24]. Besides, it is a more convenient format to compare with experimental results. Therefore, we assume the following relationship:

$$\Gamma = \alpha_1 g + \delta_1 \tag{35}$$

$$J_0 = \alpha_2 g + \delta_2. \tag{36}$$

The complicated interplay between J_0 and Γ can be adjusted by the factors α_1, α_2, δ_1 and δ_2 in equations (35)–(36). We choose $\alpha_2 < 0$, which means that the degree of frustration enhances with the increases of the pairing coupling g. The factor δ_2 is adjusted to guarantee the AF coupling and, with the remaining factors, also to maintain the transitions and the tricritical point located at the same scale as Figures 1–3.

Figure 4 shows the phase diagram T versus g with $\Gamma = 0$. For that case, the behaviour of transition temperatures is obtained from the solution of order parameters (Eqs. (23)–(25)) together with the AT line (Eqs. (26), (27)) using only equation (36). For small g (small degree of frustration), there is a transition from paramagnetism (NP) to AF phase. Consequently, the Néel temperature decreases when g is increased. Then, in a interval of g, there is direct transition from NP to SG phase (in this case $T_g = T_f$). For large g the PAIR phase is completely dominant. At temperature $T < T_g$, the situation is richer when g increases as consequence of the RS lack of stability. The solutions found are AF at small g and SG at some interval of g as before. However, in a very small range of g, a mixed phase AF+SG intermediated between

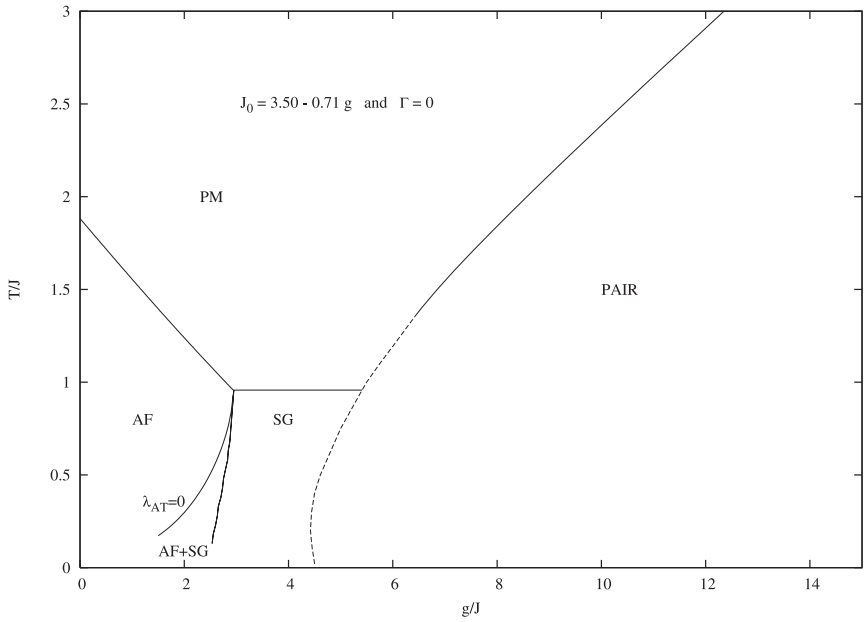

Fig. 4. Phase diagram T/J versus g/J builds for the relation $J_0 = 3.50 - 0.71g$ and $\Gamma = 0$. The dashed line indicates a first-order phase transition while the full lines indicate second-order phase transitions.

AF and the SG phases appears. Then, after the sequence of second order transitions AF-AF+SG-SG, there is a first order boundary between SG and the PAIR phase. The location of the tricritical point T_{tricl} is not changed as compared with phase diagrams shown in Figures 1 and 2 when $\Gamma = 0$.

Figures 5, 6 show the solution for the order parameters when the transverse field Γ is also tunned by equation (35). The numerical factors α_1 and δ_1 can be used to adjust the strength of the transverse field as g increases. In Figure 5, Γ affects the transition line $T_{\rm N}$ and particularly T_g, which moves downwards when g increases. The sequence of phases at lower temperature is preserved as in Figure 4. However, Γ is not strong enough to lead T_g to a QCP. On the other hand, the behaviour of the PAIR phase boundary $T_1(g)$ is affected as in Figures 1–3 in which T_{tricl} moves upward when Γ increases. In particular, it is possible to find one metastable SG solution into the PAIR phase below T_g which keeps going downward. Figure 6 displays the situation where α_1 and δ_1 are adjusted to enhance the strength of Γ as compared with Figure 5. For that case, the spin flipping induced by Γ is strong enough to lead T_g to a QCP while the T_{tricl} is obtained at a larger value than before. For both cases of Figures 5 and 6, the tunning of Γ still preserves the sequence of phases AF-AF+SG-SG at low temperature likewise the case $\Gamma = 0$ for a certain range of g.

4 Conclusions

In the present paper, we have analysed the competition among antiferromagnetism (AF), spin glass (SG) and pairing formation phase (PAIR) in the presence of a quantum tunneling mechanism. The two-sublattice model used is composed by a Gaussian random interlattice Ising interaction (with mean J_0 and standard deviation J) [26], an intralattice pairing interaction with an applied transverse field Γ. The partition function is calculated in the functional integral formalism in which the spin operators are given by bilinear combinations of Grassmann fields [19,20,24]. The saddle-point Grand Canonical potential is obtained within of static approximation (SA), the replica symmetry (RS) ansatz and in the half-filling. Particularly, the use of SA is justified because our main interest is to study in detail the phase boundaries among AF, SG and PAIR phases when the spin flipping is activated by a transverse field Γ.

In the mean field theory presented, the phase transitions of the fermionic system defined in equation (1) appear related with pairing and magnetic internal fields for each sublattice p. The magnetic one h_p ($p = A$, B) has a random and AF components. In particular, the AF part of h_p depends on the sublattice magnetization $m_{p'}$ as well as the random part is associated with the replica non-diagonal SG order parameter $q_{p'}$ and also with $\overline{\chi}_{p'} = \overline{q}_{p'} - q_{p'}$ ($\overline{q}_{p'}$ is the replica diagonal SG order parameter), where $p \neq p'$. In contrast, the pairing internal field applied in the sublattice p depends on the PAIR order parameter η_p. Furthermore, there is the presence of Γ which tunes the spin flipping and, hence tends to suppress any kind of magnetic phase. The pairing formation is also affected, as it can be clearly seen in Figure 3.

The solutions for q_p, $\overline{\chi}_p$, m_p and η_p (PAIR order parameter) are located in a parameter space given (in units of J) by J_0, Γ and g (the strength of the pairing interaction). Figures 1, 2 and 3 show the phase diagrams for several cuts in the previous space.Thus, it is possible to identify how each parameter can favour one particular solution for a given temperature. Another important point is to locate the Almeida-Thouless line (T_f) in such space. To take a typical case, in Figure 2, we present the phase

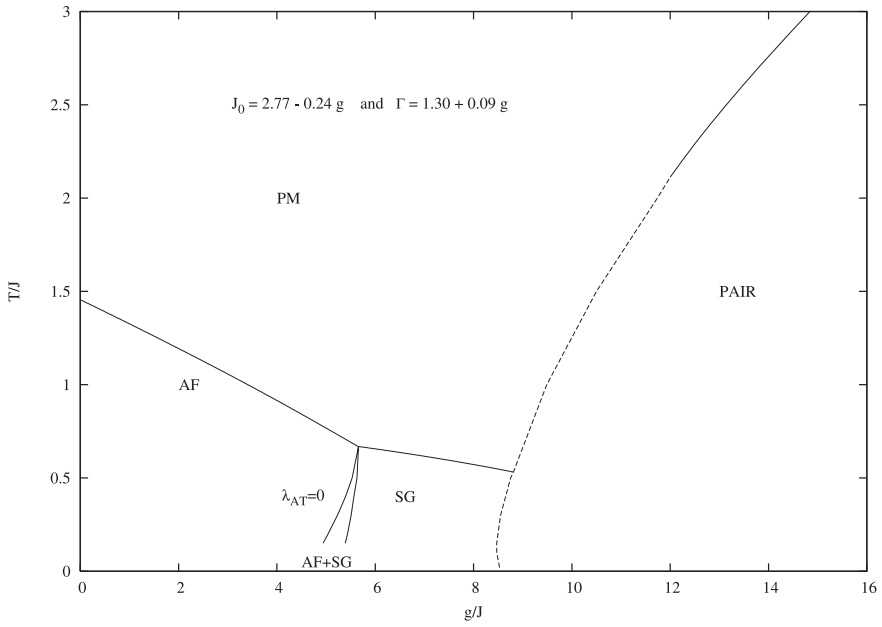

Fig. 5. Phase diagram T/J versus g/J obtained from a relationship among J_0/J, Γ/J and g/J ($J_0 = 2.77 - 0.24g$ and $\Gamma = 1.30+0.09g$). It is used the same convention as Figure 1 for the transition lines.

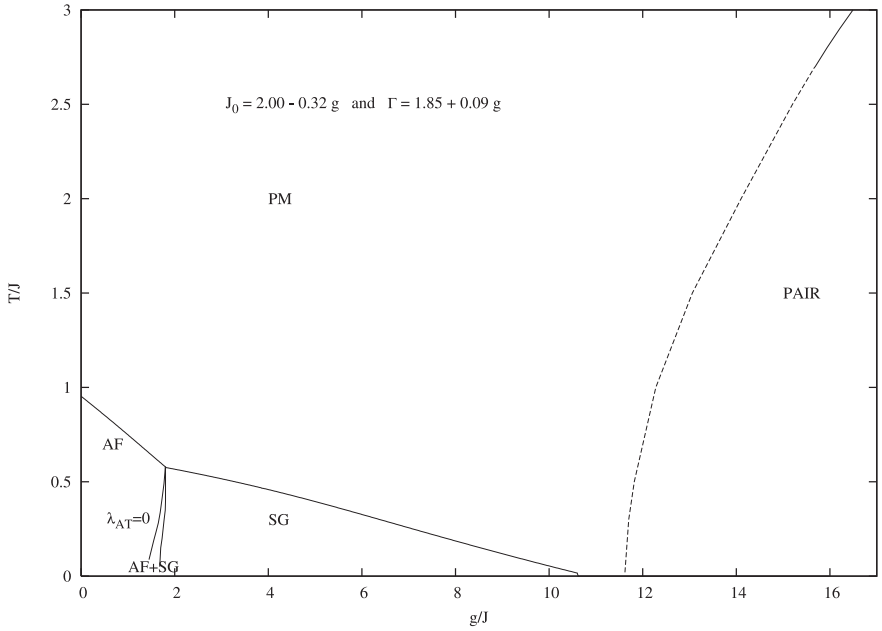

Fig. 6. Phase diagram T/J versus g/J for the relations $J_0 = 2.00 - 0.322g$ and $\Gamma = 1.85 + 0.09g$. The same convention as Figure 1 is used for the transition lines.

diagram temperature *versus* g for a $J_0 = 1.7J$ and $\Gamma = 0$ and J. For lower g, the magnetic solutions are dominant with a sequence of second order phase transitions AF, a mixed phase AF+SG and SG at lower temperature. For larger g, the local pairing is dominant. Actually, the PAIR phase boundary $T_1(g)$ has a complex nature with the presence of a tricritical point T_{trict} which is quite dependent on the transverse field Γ (see Eqs. (31, 32)).

In the phase diagrams 4, 5 and 6, we propose a relationship between the parameters J_0 and Γ with g (see Eqs. (35, 36)) based on the original derivation of the model given in equation (1) (see Ref. [19]). This procedure allows to compare our results with the phase boundaries found in experimental phase diagrams. For instance, there are some similarities between the experimental situation for $Y_{1-x}Ca_xBa_2Cu_3O_6$ and the phase diagram shown in Figure 5 as well as between $U_{1-x}La_xPd_2Al_3$ and the one shown in Figure 6, if it is possible to associate the doping in those physical systems with the parameter g. For the first case, similarities such as the sequence of phases and, in particular, the presence of SG mixed with an AF background. In terms of the present model, the decrease of experimental SG temperature transition T_g could be explained by the presence of quantum spin flipping mechanism which is not strong to lead T_g towards a QCP. For the second one, there are also similarities not only between the phase boundaries, but also with the behaviour of T_g which is depressed to a QCP.

To conclude, in this work we studied the thermodynamics of the model given in equation (1). Our goal is to obtain the corresponding phase boundaries and, then to mimic the global phase diagram of physical systems as $Y_{1-x}Ca_xBa_2Cu_3O_6$ and $U_{1-x}La_xPd_2Al_3$. As last remarks it should be noticed the role of $\overline{\chi}_p$, which carries the effects of disorder even at $T > T_g$, to determine the PAIR phase boundary $T_1(g)$. In the case $T > T_g$, $\overline{\chi}_p$ is equal to the replica diagonal SG order parameter $\overline{q}_p$. In Figure 6, because of the presence of QCP, this identity is true for the entire range of temperature after the QCP. It is well known that $\overline{q}_p$ can be written in terms of the site occupation in the sublattices [33]. At the same time, the nature of $T_1(g)$ depends deeply on the transverse field Γ. This arises the question how the phase boundaries in the present problem would be affected by the interplay between the chemical potential μ and Γ in situations like those shown in Figures 5 and 6. It is also important to remark that the precise location of the phase boundaries below T_f needs RSB spin glass solutions, as for instance the boundary between SG and mixed phase and the first-order transition between SG (or mixed phase) and PAIR phase [21]. The study of the situation where $\mu \neq 0$ and the implementation of RSB will be object of a future work.

This work was partially supported by the Brazilian agencies CNPq (Conselho Nacional de Desenvolvimento Científico e Tecnológico) and CAPES (Coodenação de Aperfeiçoamento de Pessoal de Nivel Superior).

References

1. F. Steglich, Physica B **359–361**, 326 (2005)
2. P.A. Lee, N. Nagaosa, X.G. Wen, Rev. Mod. Phys. **78**, 17 (2006); M.R. Norman, C. Pepin, Rep. Prog. Phys. **66**, 1547 (2003)
3. E. Dagotto, Science **39**, 257 (2005)
4. E. Miranda, V. Dobrosavljevic, Phys. Rev. Lett. **78**, 290 (1997); E. Miranda, V. Dobrosavljevic, Phys. Rev. Lett. **86**, 264 (2001)
5. A.H. Castro Neto, B.A. Jones, Phys. Rev. B **62**, 14975 (2000)
6. A. Otop, S. Sullow, M.B. Maple, A. Weber, E.W. Scheidt, T.J. Gortenmulder, J.A. Mydosh, Phys. Rev. B **72**, 024457 (2005)
7. R.P. Dickey, E.J. Freeman, V.S. Zapf, P.-C. Ho, M.B. Maple, Phys. Rev. B **68**, 144402 (2003); V.S. Zapf, E.J. Freeman, R.P. Dickey, P.-C. Ho, M.B. Maple, Physica B **312–313**, 448 (2002)
8. V.S. Zapf, R.P. Dickey, E.J. Freeman, C. Sirvent, M.B. Maple, Phys. Rev. B **65**, 024437 (2002)
9. H. Spille, M. Winkelmann, U. Ahlheim, C.D. Bredl, F. Steglich, P. Haen, J.M. Mignot, J.L. Tholence, R. Tournier, J. Magn. Magn. Mater. **76/77**, 539 (1988)
10. Ch. Niedermayer, C. Bernhard, T. Blasius, A. Golnik, A. Moodenbaugh, J.I. Budnick, Phys. Rev. Lett. **80**, 3843 (1998); C.E. Stronach, D.R. Noakes, X. Wan, Ch. Niedermayer, C. Bernhard, E.J. Ansaldo, Physica C **311**, 19 (1999); Ch. Niedermayer, C. Bernhard, T. Blasius, A. Decker, A. Golnik, Hyp. Int. **105**, 131 (1997)
11. F.C. Chou, N.R. Belk, M.A. Kastner, R.J. Biergenau, A. Aharony, Phys. Rev. Lett. **75**, 2204 (1995)
12. V.M. Galitski, A.I. Larkin, Phys. Rev. B **66**, 064526 (2002)
13. N. Hasselmann, A.H. Castro Neto, C. Morais Smith, Phys. Rev. B **69**, 014424 (2004)
14. V. Juricic, L. Benfatto, A.O. Caldeira, C. Morais Smith, Phys. Rev. Lett. **92**, 137202 (2004)
15. A. Theumann, B. Coqblin, S.G. Magalhaes, A.A. Schmidt, Phys. Rev. B **63**, 054409 (2001)
16. M. Kiselev, K. Kikoin, R. Oppermann, Phys. Rev. B **65**, 184410 (2002)
17. G. Alvarez, M. Mayr, A. Moreo, E. Dagotto, Phys. Rev. B **71**, 014514 (2005)
18. M.B. Maple, Physica C **341–348**, 47 (2000)
19. S.G. Magalhaes, A. Theumann, Eur. Phys J. B **9**, 5 (1999)
20. S.G. Magalhaes, A.A. Schmidt, Phys. Rev. B **62**, 11686 (2000)
21. H. Feldmann, R. Opermann, Eur. Phys. J. B **10**, 429 (1999)
22. M.J. Nass, K. Levin, G. Grest, Phys. Rev. B **23**, 1111 (1981)
23. A.J. Bray, M.A. Moore, J. Phys. C **13**, L655 (1980)
24. S.G. Magalhaes, F.M. Zimmer, Eur. Phys. J. B **43**, 187 (2005); F.M. Zimmer, S.G. Magalhaes, Physica C **408**, 398 (2004)
25. F.M. Zimmer, S.G. Magalhaes, Physica A **359**, 380 (2006)
26. I. Ya. Korenblit, E.F. Shender, Sov. Phys. JETP **62**, 1030 (1985)
27. D. Sherrington, S. Kirkpatrick, Phys. Rev. Lett. **35**, 1972 (1975); S. Kirkpatrick, D. Sherrington, Phys. Rev. B **17**, 4384 (1978)
28. J. Ye, S. Sachdev, N. Read, Phys. Rev. Lett. **70**, 4011 (1993); N. Read, S. Sachdev, J. Ye, Phys. Rev. B **52**, 384 (1995)
29. J.R.L. de Almeida, D.J. Thouless, J. Phys. A: Math. Gen. **11**, 983, (1978)
30. R. Oppermann, D. Sherrington, Phys. Rev. B **67**, 245111 (2003); R. Oppermann, B. Rosenow, Phys. Rev. B **60**, 1035 (1999)
31. S.K. Ghatak, D. Sherrington, J. Phys. C **10**, 3149 (1977)
32. I.P. Castillo, D. Sherrington, Phys. Rev. B **72**, 104427 (2005)
33. R. Oppermann, A. Muller-Groeling, Nuclear Phys. B **401**, 507 (1993)